

β^+ decay of ^{18}Ne and the ft value of the $0^+ \rightarrow 0^-$ branch

A. M. Hernandez and W. W. Daehnick

Nuclear Physics Laboratory, University of Pittsburgh, Pittsburgh, Pennsylvania 15260

(Received 4 January 1982)

The $^{18}\text{Ne} \rightarrow ^{18}\text{F}$ β decay was studied by measuring the ^{18}F deexcitation γ rays relative to the dominant superallowed $0^+ \rightarrow 0^+$ (1042 keV) branch. The ratio of the intensity of the 0^- (1081 keV) deexcitation γ ray relative to the 1042 keV deexcitation was found to be $(2.97 \pm 0.22) \times 10^{-4}$. An absolute β branch $I_\beta = (2.14 \pm 0.26) \times 10^{-3}\%$ and $ft = (0.99 \pm 0.12) \times 10^7$ sec for the $0^+ \rightarrow 0^-$ β decay branch were deduced. This value together with the existing result on the parity mixing of the 0^+ , 0^- doublet in ^{18}F suggests $|F_\pi| = (0.4 \pm 1.1) \times 10^{-6}$. The absolute value for the $0^+ \rightarrow 1^+$ (1700 keV) β branch was deduced as $I_\beta = (0.183 \pm 0.006)\%$ and $ft = (3.19 \pm 0.12) \times 10^4$ sec.

[RADIOACTIVITY ^{18}Ne [from $^{16}\text{O}(^3\text{He}, n)$], measured E_γ , I_γ ; deduced]
 ft values, F_π limit.

I. INTRODUCTION

The $0^+ \rightarrow 0^-$, $\Delta T = 1$ transition rates are of interest because they are relatively strongly and directly related to neutral-weak-current theories.¹ In this situation, the one-pion-exchange process is expected to dominate over other, shorter range processes, and effects resulting from the parity nonconserving (PNC) nucleon-nucleon force will become more easily calculable and detectable. The predictions for the $\Delta T = 1$ part of the PNC interaction are quite different for the Cabbibo and Weinberg-Salam models of the weak interaction.² The latter predicts a relative enhancement by an order of magnitude in PNC effects, e.g., for parity mixing in nuclear states, which should provide a good way to distinguish between these different weak interaction theories.

It has been pointed out^{2,3} that ^{18}F is a good candidate for studying the $\Delta T = 1$ PNC nucleon-nucleon interaction, because the closeness (39 keV) of the low-lying 0^+ , 0^- doublet should give rise to parity mixing which manifests itself in the measurable circular polarization of the 0^- (1081 keV) deexcitation γ rays. The knowledge of this polarization permits a direct determination of the matrix element $\langle 0^- | H_{\text{PNC}} | 0^+ \rangle$, which can be related to the parameters of the weak interaction, e.g., by the use of reliable shell model wave functions.³ The circular polarization of the 1081 keV γ ray has been measured³ to be $P_c(1081) = (-0.7 \pm 2.0) \times 10^{-3}$. This value should be compared with the Cabbibo

model prediction of $P_c = 0.36 \times 10^{-3}$ [Ref. 2(a)] and with the Weinberg-Salam model predictions, either $P_c = 5.7 \times 10^{-3}$, as given in Ref. 2(a), or $P_c = (5.94_{-0.62}^{+0.50}) \times 10^{-3}$, as given in Ref. 2(b). These calculations are subject to uncertainties in the nuclear wave functions as well as in the PNC potential assumed. Hence a study of the PNC potential could be much more informative if the uncertainty resulting from the computed nuclear wave functions could be reduced. It has now been shown by Haxton⁴ that the simultaneous knowledge of the ft value for the $^{18}\text{Ne}(0^+) \rightarrow ^{18}\text{F}(0^-, 1081 \text{ keV})$ β decay can yield the information necessary to free the conclusions based on the results of Ref. 3 from the uncertainties associated with the calculated mass 18 wave functions. Adelberger *et al.*⁵ have published a first such measurement of this weak decay branch and have deduced a value for the PNC interaction parameter of $|F_\pi| = (0.5 \pm 1.3) \times 10^{-6}$. Because of its considerable interest, the study reported here aimed at checking and possibly improving the accuracy of the ft value reported in Ref. 5.

II. EXPERIMENTAL PROCEDURE

^{18}Ne , with a half-life⁶ of $T_{1/2} = 1.672 \pm 0.004$ sec, was produced by the reaction $^{16}\text{O}(^3\text{He}, n)^{18}\text{Ne}$. Oxygen gas of natural isotopic composition (99.76% ^{16}O) was bombarded with ^3He beams of ≤ 600 nA from the Pittsburgh tandem Van de Graaff. The ^{16}O gas was contained in a Ta-lined cylindrical cell

of 0.5 cm inner diameter and 13 cm length with $3.81 \mu\text{m}$ thick Havar beam entrance and exit foils, which could tolerate pressures up to 5 atm. The ^{16}O gas containing the radioactive reaction product ^{18}Ne was circulated through a 4.5 m long plastic capillary to a plexiglass cell in the shielded counting area at a calculated flow rate of about $6.7 \text{ cm}^3 \text{ atm/sec}$. It then returned through a second capillary and a cold trap (kept at dry ice temperature) to the compressor which fed the target cell.⁷ The target contained 2.6 cm^3 of gas at typically 3.3 atm, whereas the counting cell was typically kept at 2.5 atm and had various geometries, all of them with a volume several times that of the target cell. The 4.5 m line from the target to the counting cell contained a 20 cm section of stainless steel capillary (at room temperature) which served to trap most of the F activities produced in the $(\text{O} + ^3\text{He})$ reactions. The (dry ice) cold trap in the return line was found to accumulate less of the fluorine activity. It seemed to trap significant amounts of water. (In the present experiment, this trap could not be kept at liquid nitrogen temperatures because this would dramatically decrease the amount of circulating oxygen.) For the decay scheme of ^{18}Ne , see Fig. 1.

Experiments were performed at $E_{\text{He}^3} = 15$ and 18 MeV, which differed in several aspects. For the 15 MeV runs, the gas target was kept at 50 mg/cm^2 of ^{16}O (behind 3.3 mg/cm^2 of Fe). In one experiment, the counting cell was small and was mounted close to the anti-Compton shield of the Ge(Li) detector (approximately in the position of the lead collimator in Fig. 2). In the other experiments the geometry shown in Fig. 2 was used. In runs with the higher

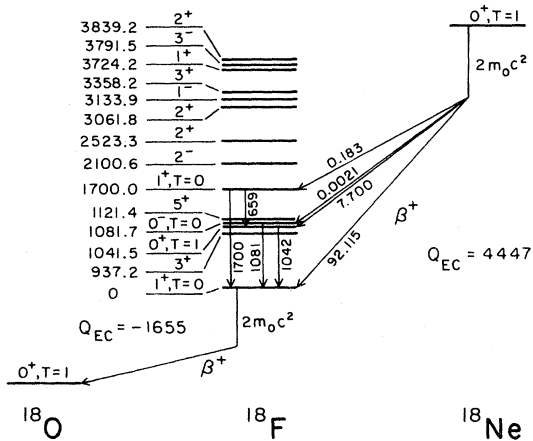


FIG. 1. Decay scheme of ^{18}Ne . The quoted β branches are based on present work.

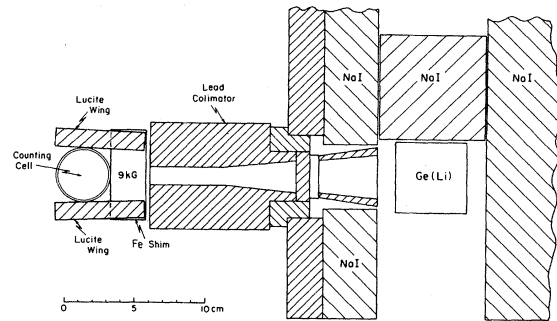


FIG. 2. Schematic view of the detector setup.

beam energy, the target thickness was increased to about 60 mg/cm^2 . This resulted in a higher decay rate in the counting cell, which was desirable because the detector "saw" only a portion of the cell and also subtended a smaller solid angle than in the 15 MeV run. The flow system was "tuned" to preferentially detect activities with half-lives of $1 < T_{1/2} < 2$ sec and it is seen in Fig. 3 that the ^{18}Ne decay spectrum dominates all other activities. The largest amount of beam related background comes from the decay of ^{14}O . Much smaller amounts of ^{19}O and ^{20}F are seen. The remainder of the peaks constitute long-life background from the room, the Pb shielding, and the large NaI anti-Compton shield. Lifetime measurements furthermore indicated the presence of considerable amounts of ^{18}F (110 min), and smaller amounts of ^{17}F (66 sec) and ^{15}O (124 sec). These β^+ emitters did not particularly hinder our measurements since they all decay to the ground states of their daughters. Some continuous background is produced by those of the ^{17}F and ^{15}O positrons which decay in flight; however, the major portion of the background near the 1081 and 1700 keV peaks comes from in-flight decay of the ^{18}Ne and ^{14}O positrons and from the Compton region of the ^{14}O , 2313 keV peak.

Although we use a very different gas handling system, we see in Fig. 3 a γ spectrum very similar to that given in Ref. 5. The major difference is that the ratio of the Compton and annihilation continuum in Fig. 3 to the peaks of interest is lower than in Ref. 5 by about a factor of 5. Consequently, the weak background peaks as well as the ^{18}Ne peaks are more visible. With the possible exception of the more pronounced ^{14}O peaks, the use of higher ^3He beam energies was not expected to, and does not seem to, have introduced new background peaks.

A weak, unidentified γ peak is seen at $E_\gamma = 1164$ keV, for both the 15 and 18 MeV runs. This peak is

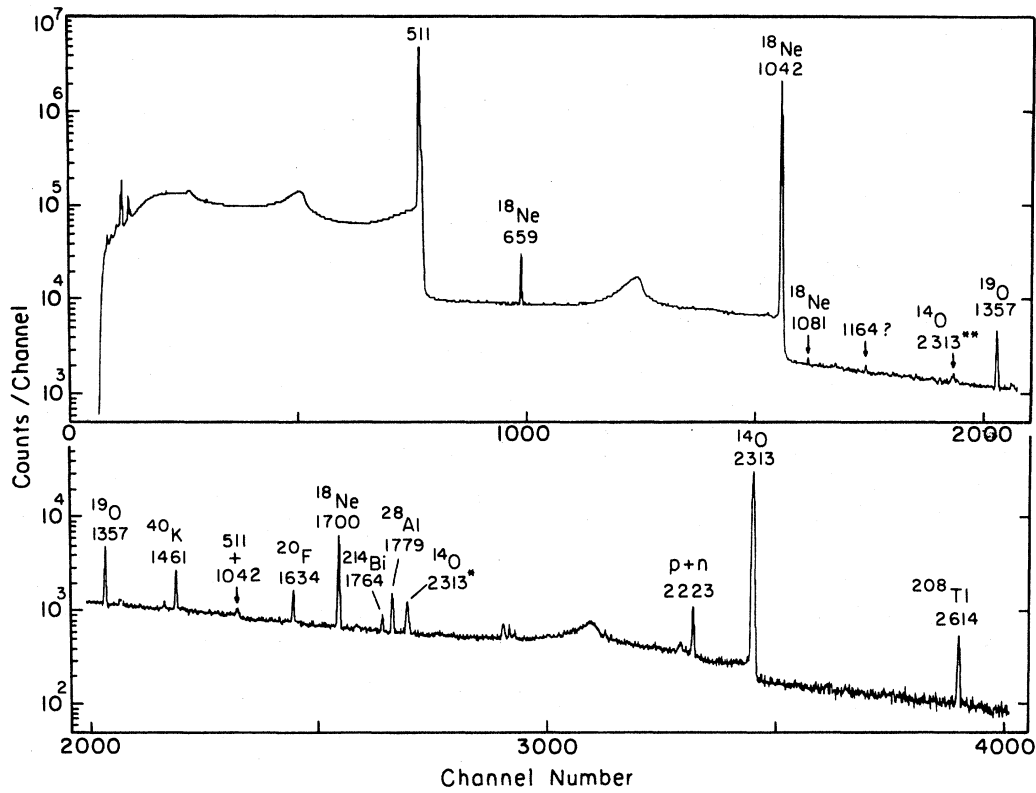


FIG. 3. Semilog plot of the γ ray spectrum taken at $E_{3\text{He}} = 18$ MeV with anti-Compton shield and positron deflector.

not part of the room background, and seems proportional to the ^{18}Ne decays. An 1164 keV line is known from ^{62}Co decay and the $^{62}\text{Ni}(^3\text{He},3p)^{62}\text{Co}$ reaction (in the gas target foils) is energetically possible. However, ^{62}Co decay should also show a second, slightly more intense peak at 1173 keV which is not present. An 1164 keV transition is possible in ^{18}F [2101 keV (2^-) \rightarrow 937 keV (3^+)], but not previously reported. It is doubtful that the 2^- level at 2101 would be fed with any appreciable strength in ^{18}Ne β decay. [In principle, a weak electron capture branch should feed the higher lying 3.724 (1^+) level in ^{18}F ; however, this level does not feed the 2101 keV state appreciably.⁸]

The significant reduction of the continuum background is largely due to our use of an anti-Compton shield for the Ge(Li) detector.⁷ The remainder is attributable to the highly collimated field of view for the detector, as evident from Fig. 2, and to the use of magnetic deflection for positrons, which contributed an improvement factor of about 1.4. Of all regions where positrons can annihilate, only a portion of the thin counting cell walls and the gas itself are visible to the detector. The 9 kG B field applied between gas cell and collimator primarily prevents

positrons from moving towards the γ detector and thus from annihilating in flight in the surrounding lead. (Use of a B field in order to reduce annihilation background has been made before at Princeton and by Bowles *et al.*⁹) Other aspects of the experiment are conventional. A 0.95 cm thick Pb absorber was placed in front of the Ge(Li) detector in order to differentially attenuate low energy radiation. Pulse pileup rejection was used. Gas charges and capillary lines were replaced at intervals of about 6 and 24 h in order to prevent the buildup of impurities and deposits. Energy calibrations and linearity checks were made with a ^{56}Co source; however, the relative detector efficiency was calibrated with activities produced in the gas target by means of the $^{20}\text{Ne}(^3\text{He},n)^{22}\text{Mg}$ and $^{32}\text{S}(^3\text{He},p)^{34}\text{Cl}^m$ reactions. These gaseous activities can be expected to fill the "extended" counting cell more like the ^{18}Ne gas had. They yield results that differ somewhat from those of a point source placed at the center of the cell. Relative to the 1042 keV peak the 1081 keV efficiency is not measurably affected; however, a 10% difference was found for the 1700 keV point. The true value of the efficiency would be somewhere in between the results obtained with

these two different calibrations. Calculated corrections to the point source calibration suggest that the gas calibration gives the better approximation for the ^{18}Ne activity. However, some uncertainty remains, as ^{22}Mg and ^{34}Cl are reactive elements and may deposit to some degree on the Lucite cell walls.

III. RESULTS AND ANALYSIS

Four independent runs were made. Three of them, two at 18 MeV and one at 15 MeV, used the detection geometry shown in Fig. 2. In addition, one run at 15 MeV was performed as mentioned above with a different geometry and no magnetic field. In all four cases, the measured values agree with each other well within their computed uncertainties. In the semilog spectrum of Fig. 3 peaks attributed to room background and impurity activities are indicated. Figure 4 shows, for the same spectrum, a linear plot of the region of the weak 1081 keV peak; there is no appreciable room background in this region.

In Table I, data for the four runs are combined using $1/\sigma^2$ weighting, and energies and relative intensities for the ^{18}Ne - ^{18}F γ transitions are given. For comparison, results of earlier work are also listed. Our measurements for the 659 and 1700 keV γ ray intensities agree, within their uncertainties, with all previous results, which had low statistics.^{10,11} A comparison with the more recent work of Adelberger *et al.*⁵ shows that our results for the intensities of the 1700 keV branches are smaller, although only by about 1.6 standard deviations. Our result for the 1081 keV γ ray intensity, however, is significantly higher than the value reported in Ref. 5, where background subtraction may have been a problem.

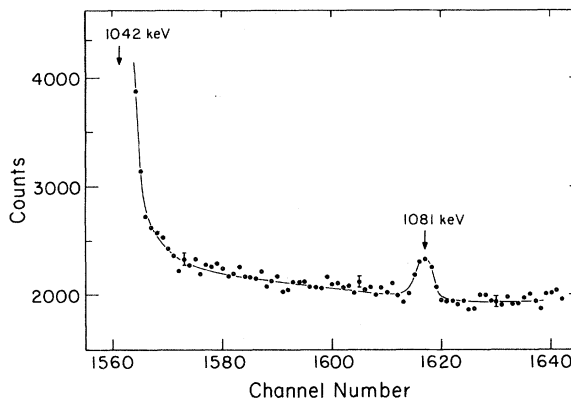


FIG. 4. Linear plot of the spectrum shown in Fig. 3, near the 1081 keV region. The bars show the typical statistical errors. There are no measurable room background peaks in the region shown.

In order to calculate the ^{18}Ne β^+ branching ratios we must subtract from the 1042 and 1081 keV γ intensities the contributions due to the deexcitation of the 1700 keV state through those levels. For the 1042 keV level this is simply the measured intensity of the 659 keV γ ray. The γ feeding to the 1081 keV level from the 1700 keV level has an upper limit of 0.2% of the total γ intensity of the 1700 keV state deexcitation⁸ (i.e., $1.69 + 0.646$ from Table I). Then the maximum contribution to the 1081 keV γ intensity due to $1700 \rightarrow 1081$ feeding is $\leq 0.467 \times 10^{-2}$, and for our computation this feeding was taken as $(0.234 \pm 0.234) \times 10^{-2}$. The resulting ^{18}Ne β^+ branching ratios relative to the (renormalized) 1042 keV transition are listed in column 2 of Table II. Using the absolute 1042 keV γ ray intensity ratio relative to the total β^+ decay strength of $(7.83 \pm 0.21)\%$, given in Ref. 6, these results

TABLE I. ^{18}F deexcitation γ intensities observed for $^{18}\text{Ne} \rightarrow ^{18}\text{F}$ β^+ decay and comparison with prior work.

E_γ (keV)	659.2 \pm 0.3	1041.5 \pm 0.3	1080.7 \pm 0.5	1699.9 \pm 0.3
E_{He^3} = 15 MeV, geom 1, $B = 0$	1.65 \pm 0.07	100	$(2.96 \pm 0.46) \times 10^{-2}$	0.643 \pm 0.010 ^a
E_{He^3} = 15 MeV, geom 2, $B = 9$ kG	1.77 \pm 0.11	100	$(2.86 \pm 0.59) \times 10^{-2}$	0.658 \pm 0.023 ^a
E_{He^3} = 18 MeV, geom 2, $B = 9$ kG	1.75 \pm 0.10	100	$(3.07 \pm 0.38) \times 10^{-2}$	0.653 \pm 0.022 ^a
E_{He^3} = 18 MeV, geom 2, $B = 9$ kG	1.69 \pm 0.07	100	$(2.93 \pm 0.39) \times 10^{-2}$	0.636 \pm 0.017 ^a
Average, this work:	1.69 \pm 0.04	100	$(2.97 \pm 0.22) \times 10^{-2}$	0.646 \pm 0.021 ^b
Ref. 5	1.75 \pm 0.05	100	$(1.92 \pm 0.32) \times 10^{-2}$	0.680 \pm 0.011
Ref. 10	2.1 \pm 0.3	100		0.71 \pm 0.17
Ref. 11	1.6 \pm 0.5	100		0.7 \pm 0.2

^aStatistical errors only.

^bThis error is determined primarily by the uncertainty in the Ge(Li) efficiency calibration.

TABLE II. ^{18}Ne β -decay branches to specified ^{18}F states, relative to the $0^+ \rightarrow 0^+$ (1042 keV) β decay. The absolute^a decay rates I_β calculated from the present experiment are also indicated.

E (keV) Final state	Relative intensities	I_β (%) (Absolute branch)
1041.5	100	7.70 \pm 0.21
1080.7	$(2.783 \pm 0.327) \times 10^{-2}$	$(2.14 \pm 0.26) \times 10^{-3}$
1699.9	2.376 ± 0.045	0.183 ± 0.006

^aNormalized to total β decay rate from Ref. 10.

determine an absolute branch for the β^+ decay to the 1081 keV, 0^- level of

$$I_\beta(1081) = (2.14 \pm 0.26) \times 10^{-3} \% .$$

Similarly, the result for β decay to the 1700 keV level is

$$I_\beta(1700) = (0.183 \pm 0.006) \% .$$

Based on these experimental results, the ft value for the 1081 (0^-) branch is $ft = (0.99 \pm 0.12) \times 10^7$ sec. The $\log f$ value, corrected for K capture, was taken from Ref. 12, assuming an allowed β^+ spectrum shape.⁵ This ft value is noticeably smaller than that of Ref. 5 and it seems useful to reestimate the strength of the PNC π -exchange NN interaction F_π , through the expression⁵

$$F_\pi = \frac{\langle 0^- | H_{\text{PNC}} | 0^+ \rangle}{M_N} \frac{\alpha + 1}{\alpha} \frac{g^2}{4\pi} \\ \times \frac{\pi}{2F_A} \left[\frac{(ft)_{0^+ \rightarrow 0^-}}{(ft)_{0^+ \rightarrow 0^+}} \right]^{1/2} .$$

The PNC matrix element $\langle 0^- | H_{\text{PNC}} | 0^+ \rangle$, obtained from the measured³ circular polarization of the 1081 keV γ transition from the 0^- state to the ground state, is (0.13 ± 0.36) eV. The ratio of the two body to the one-body β decay matrix elements α is nearly constant, independent of the nuclear

structure⁴ ($\alpha \approx 0.67$). We take the strong πNN coupling constant⁴ $g = 13.45$ and the axial form factor⁴ $F_A = -1.23$. Inserting⁶ $(ft)_{0^+ \rightarrow 0^+} = 2857 \pm 80$ sec and our measured $(ft)_{0^+ \rightarrow 0^-}$ value we find $|F_\pi| = (0.4 \pm 1.1) \times 10^{-6}$.

IV. CONCLUSIONS

Our measurement for the ^{18}Ne $0^+ \rightarrow 0^-$ beta branching ratio was found to be about 50% larger than that given in Ref. 5 and, consequently, the value deduced for the PNC interaction parameter F_π is about 25% smaller. As a result, the allowed range for F_π has been narrowed from $|F_\pi| \leq 1.8 \times 10^{-6}$ to $|F_\pi| \leq 1.5 \times 10^{-6}$. Freed from the uncertainties of the nuclear structure calculations this experimental range for F_π continues to include the value $F_\pi = 1.08 \times 10^{-6}$ deduced from an analysis of hyperon decays with the use of the Weinberg-Salam model of the weak interaction, and $[\text{SU}(6)]_w$ and the quark model of hadron structure.¹³ This "best value" of F_π is the value which was used by Haxton *et al.* [Ref. 2(b)] to compute the "Weinberg-Salam" value $P_c = 5.94 \times 10^{-3}$ for the circular γ polarization. As quoted in the Introduction, this calculation was about 2.6 standard deviations above the experimental value for P_c and hence in conflict with observation. It now seems that a major part of this disagreement might be attributable to the nuclear wave functions used in Ref. 2. The error in the range of F_π attributable to the remaining uncertainty in the $0^+ \rightarrow 0^-$ β branch is about 5%; hence, it seems that the test for F_π can only be sharpened if the value for P_γ from Ref. 3 can be improved. Thus, although we have found reason to significantly revise $(ft)_{0^+ \rightarrow 0^-}$, the considerations and conclusions given by Adelberger *et al.*⁵ appear still valid.

ACKNOWLEDGMENTS

The authors would like to acknowledge the assistance in the data taking of Dr. J. M. Niedra, Dr. M. J. Spisak, A. El Ganayni, and J. H. Chang. A. El Ganayni constructed much of the gas handling apparatus and J. H. Chang improved the beam transport system. This work was supported by a grant of the National Science Foundation.

- ¹K. Kubodera, J. Delorme, and M. Rho, Phys. Rev. Lett. 40, 755 (1978).
- ^{2(a)}M. Gari, J. B. McGrory, and R. Offermann, Phys. Lett. 55B, 277 (1975).
- ^(b)W. C. Haxton, B. F. Gibson, and E. M. Henley, Phys. Rev. Lett. 45, 1677 (1980).
- ³C. A. Barnes, M. M. Lowry, J. M. Davidson, R. E. Marrs, F. B. Morinigo, B. Chang, E. G. Adelberger, and H. E. Swanson, Phys. Rev. Lett. 40, 840 (1978).
- ⁴W. C. Haxton, Phys. Rev. Lett. 46, 698 (1981).
- ⁵E. G. Adelberger, C. D. Hoyle, H. E. Swanson, and R. D. Von Lintig, Phys. Rev. Lett. 46, 695 (1981).
- ⁶F. Ajzenberg-Selove, Nucl. Phys. A300, 1 (1978).
- ⁷A. M. Hernandez and W. W. Daehnick, Phys. Rev. C 24, 2235 (1981).
- ⁸C. Rolfs, H. P. Trautvetter, R. E. Azuma, and A. E. Litherland, Nucl. Phys. A199, 289 (1973)
- ⁹T. J. Bowles *et al.*, Bull. Am. Phys. Soc. 26, 568 (1981).
- ¹⁰J. C. Hardy, H. Schmeing, J. S. Geiger, and R. L. Graham, Nucl. Phys. A246, 61 (1975).
- ¹¹E. Aslanides, F. Jundt, and A. Gallmann, Nucl. Phys. A152, 251 (1970).
- ¹²N. B. Gove and M. J. Martin, Nucl. Data Tables 10, 205 (1971).
- ¹³B. Desplanques, J. F. Donoghue, and B. R. Holstein, Ann. Phys. (Paris) 124, 449 (1980).